

Proton-proton correlations in distinguishing the two-proton emission mechanism of ^{23}Al and ^{22}Mg

D. Q. Fang,^{1,*} Y. G. Ma,^{1,†} X. Y. Sun,¹ P. Zhou,¹ Y. Togano,² N. Aoi,² H. Baba,² X. Z. Cai,¹ X. G. Cao,¹ J. G. Chen,¹ Y. Fu,¹ W. Guo,¹ Y. Hara,³ T. Honda,³ Z. G. Hu,⁴ K. Ieki,⁵ Y. Ishibashi,⁵ Y. Ito,⁵ N. Iwasa,⁶ S. Kanno,² T. Kawabata,⁷ H. Kimura,⁸ Y. Kondo,² K. Kurita,³ M. Kurokawa,² T. Moriguchi,⁵ H. Murakami,² H. Ooishi,⁵ K. Okada,³ S. Ota,⁷ A. Ozawa,⁵ H. Sakurai,² S. Shimoura,⁷ R. Shioda,³ E. Takeshita,² S. Takeuchi,² W. D. Tian,¹ H. W. Wang,¹ J. S. Wang,⁴ M. Wang,⁴ K. Yamada,² Y. Yamada,³ Y. Yasuda,⁵ K. Yoneda,² G. Q. Zhang,¹ and T. Motobayashi²

¹Shanghai Institute of Applied Physics, Chinese Academy of Sciences, Shanghai 201800, China

²Institute of Physical and Chemical Research (RIKEN), Wako, Saitama 351-0198, Japan

³Department of Physics, Rikkyo University, Tokyo 171-8501, Japan

⁴Institute of Modern Physics, Chinese Academy of Sciences, Lanzhou 730000, China

⁵Institute of Physics, University of Tsukuba, Ibaraki 305-8571, Japan

⁶Department of Physics, Tohoku University, Miyagi 980-8578, Japan

⁷Center for Nuclear Study (CNS), University of Tokyo, Saitama 351-0198, Japan

⁸Department of Physics, University of Tokyo, Tokyo 113-0033, Japan

(Received 6 August 2016; revised manuscript received 11 September 2016; published 28 October 2016)

The proton-proton momentum correlation functions $[C_{pp}(q)]$ for the kinematically complete decay channels $^{23}\text{Al} \rightarrow p + p + ^{21}\text{Na}$ and $^{22}\text{Mg} \rightarrow p + p + ^{20}\text{Ne}$ have been measured at the RIKEN RI Beam Factory. From the very different correlation strength of $C_{pp}(q)$ for ^{23}Al and ^{22}Mg , the source size and emission time information were extracted from the $C_{pp}(q)$ data by assuming a Gaussian source profile in the correlation function calculation code (CRAB). The results indicated that the mechanism of two-proton emission from ^{23}Al was mainly sequential emission, while that of ^{22}Mg was mainly three-body simultaneous emission. By combining our earlier results of the two-proton relative momentum and the opening angle, it is pointed out that the mechanism of two-proton emission could be distinguished clearly.

DOI: [10.1103/PhysRevC.94.044621](https://doi.org/10.1103/PhysRevC.94.044621)

I. INTRODUCTION

The two-particle intensity interferometry has been extensively utilized to determine the space-time extension of particle-emitting sources in nuclear and particle physics over the past several decades [1–10]. In heavy-ion collisions, the two-particle interferometry is a well-recognized and powerful method to characterize the source of particle emission and to probe and disentangle different reaction mechanisms. In particular, this method can provide information on the space-time evolution of hot nuclei that usually decay by evaporation and/or (multi-)fragmentation. Even though a large number of experiments have been carried out to measure the two-proton correlation in nuclear fragmentation, almost no proton-proton momentum correlation function measurement has been reported for a kinematically complete decay channel. In contrast, there have been several measurements of the neutron-neutron momentum correlation function in kinematically complete decay channels for halo nuclei, such as ^{11}Li [11–13] and ^{14}Be [12], which were believed to be useful for studying the so-called dineutron structure of neutron-rich nuclei [14].

The phenomenon of two-proton emission is a very interesting but complicated process existing in the nucleus close to the proton-drip line [15–19]. The proton-proton correlation plays an important role in the emission mechanism.

There is a distinct difference in the spectra of the two-proton relative momentum (q_{pp}) and the opening angle (θ_{pp}) between the diproton emission and the two-body sequential or three-body simultaneous emission. This characteristic has been used to investigate the mechanism of two-proton emission [20,21].

The proton-rich nuclei ^{23}Al and ^{22}Mg are very important in determining some astrophysical reaction rates and have attracted a lot of attention in both astrophysics and nuclear structure studies [22–29]. Recently, we have reported the experimental results for kinematically complete measurements of two-proton emissions from two excited proton-rich nuclei, namely, $^{23}\text{Al} \rightarrow p + p + ^{21}\text{Na}$ and $^{22}\text{Mg} \rightarrow p + p + ^{20}\text{Ne}$ [30]. Based on the analysis of q_{pp} and θ_{pp} distributions of the two emitted protons, a favorable diproton emission component from the excited states around 14.044 MeV of ^{22}Mg was observed. However, no such signal was exhibited in the two-proton emission processes of the excited ^{23}Al .

As pointed out in Ref. [30], it is difficult to distinguish between the two-body sequential and three-body simultaneous emission mechanism using the above analysis. In these two mechanisms, the emission time of the two protons is quite different. For three-body simultaneous emission, the two protons are emitted almost at the same time, while the two protons are emitted one by one in sequential emission. The two-particle intensity interferometry method has been demonstrated to be a good way to extract the source size and particle emission time [31,32]. In this paper, the proton-proton momentum correlation function is studied for the three-body

*dqfang@sinap.ac.cn

†ygma@sinap.ac.cn

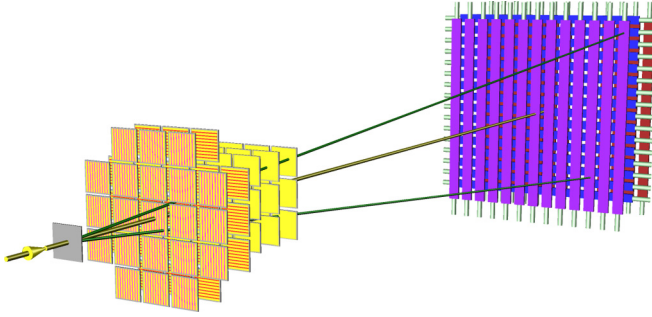


FIG. 1. The layout of detector setup. For details see the text.

decay channels $^{23}\text{Al} \rightarrow p + p + ^{21}\text{Na}$ and $^{22}\text{Mg} \rightarrow p + p + ^{20}\text{Ne}$. The size and emission time information of the source are extracted. The possibility of distinguishing sequential and three-body simultaneous emission mechanisms is investigated.

II. EXPERIMENT DESCRIPTION

The experiment was performed using the RIPS beam line at the RI Beam Factory (RIBF) operated by the RIKEN Nishina Center and the Center for Nuclear Study, University of Tokyo. A primary beam of $135A$ MeV ^{28}Si was used to produce secondary ^{23}Al and ^{22}Mg beams with incident energies of $57.4A$ MeV and $53.5A$ MeV in the center of the carbon reaction target, respectively. After the reaction target, there were five layers of silicon detectors and three layers of plastic hodoscopes as shown in Fig. 1. The first two layers of Si-strip detectors located around 50 cm downstream of the target were used to measure the emitting angle of the fragment and protons. Three layers of 3×3 single-electrode Si were used as the ΔE - E detectors for the fragment. The three layers of plastic hodoscopes located around 3 m downstream of the target were used as ΔE and E detectors for protons. The time of flight of the protons was measured by the first layer. Clear particle identifications were obtained by this setup for the kinematically complete three-body decay reactions. The momentum and emission angle for protons and the residue are determined by analyzing the detector signals. The excitation energy (E^*) of the incident nucleus was reconstructed by the difference between the invariant mass of the three-body system and the mass of the mother nucleus in the ground state. A more detailed description of the experiment can be found in Ref. [30].

III. RESULTS AND DISCUSSION

In the present study, the momentum correlation functions between two protons emitted from ^{23}Al and ^{22}Mg are studied. Experimentally, the two-proton correlation function is constructed by dividing the coincidence yield N_c by the yield of noncorrelated events N_{nc} , namely, $C_{pp}(q) = K \frac{N_c(q)}{N_{nc}(q)}$, where the relative momentum is given by $q = \frac{1}{2}|\mathbf{p}_1 - \mathbf{p}_2|$, with \mathbf{p}_1 and \mathbf{p}_2 being the momenta of the two coincident protons. The normalization constant K is determined so that the correlation function goes to unity at large values of q , where no correlation is expected.

The event-mixing technique [1] was applied to construct the background yield, i.e., by pairing a proton with a randomly chosen uncorrelated proton from different events, and then normalized to the number of two-proton correlation events in N_c . This method ensures that the uncorrelated distribution includes the same class of collisions and kinematical constraints as the numerator. It has, however, a potential problem: it may attenuate the slight correlations one wishes to measure [2] due to the existence of possible ‘‘residue correlation’’ from the initial two-proton physical correlation, which will overestimate the denominator. To eliminate this residue correlation, an iterative calculation method for the $C_{pp}(q)$ was applied and the intrinsic correlation was extracted [33]. A similar method has been first applied to the two-neutron momentum correlation function measurement for neutron-halo nuclei [13]. Here it is the first attempt to apply the correlation function analysis to two-proton emission data.

First, we looked at the two-proton correlation in the inclusive reaction channel, which is similar to the proton-proton momentum correlation function for hot nuclei. Figure 2 showed our measurements of $C_{pp}(q)$, which were obtained by the event-mixing method with an iterative calculation for the two emitted protons, without identifying the residue from the mother nucleus and using any specific E^* window. Figures 2(a) and 2(b) were the results for the inclusive channels $^{23}\text{Al} \rightarrow p + p + X$ and $^{22}\text{Mg} \rightarrow p + p + X$, respectively. In this work, the normalization factor K in calculating $C_{pp}(q)$ was determined by the $50 < q_{pp} < 100$ MeV/c data. The peak height around $q_{pp} = 20$ MeV/c reflected the strength of the correlation function. To extract the source size, theoretical calculation for $C_{pp}(q)$ was performed by using the correlation function calculation code (CRAB) [34]. A Gaussian profile was assumed for the source and the space distribution was

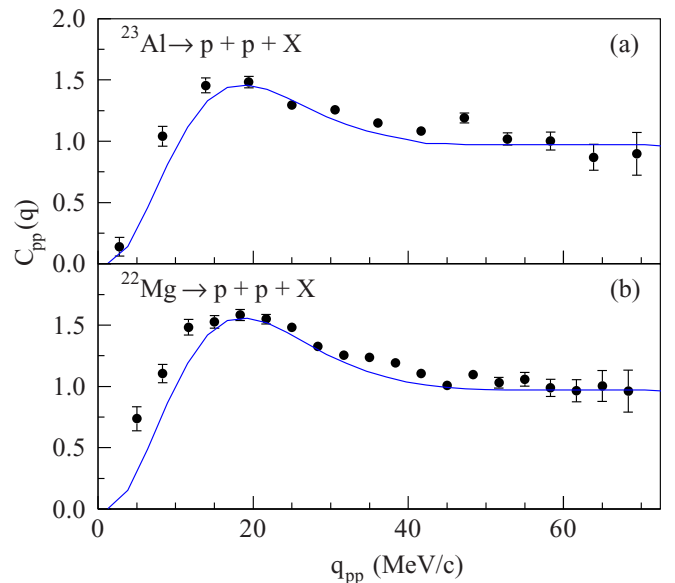


FIG. 2. The proton-proton momentum correlation function [$C_{pp}(q)$] for the reaction channels $^{23}\text{Al} \rightarrow p + p + X$ (a) and $^{22}\text{Mg} \rightarrow p + p + X$ (b). The dots are experimental data. The lines are the calculations using the CRAB code with a Gaussian source.

simulated according to the function $S(r) \sim \exp(-r^2/2r_0^2)$, with r_0 being the source size parameter. The calculations were compared with the experimental $C_{pp}(q)$ data. The source size was determined by finding the minimum of the reduced χ^2 (χ^2/ν , ν is the degree of freedom). The fit gave a source size range of $r_0 = 3.15 \sim 3.25$ fm for ^{23}Al (corresponding to the rms radius of $R_{\text{rms}} = 5.46 \sim 5.63$ fm). The uncertainty was determined from the minimum χ^2 : χ_0^2 to $\chi_0^2 + 1$. The best fit of the calculation was plotted in the figure. The obtained source size could give us information of the average distance between the two emitted protons. This size is much larger than the expected radius of the ^{23}Al nucleus. Of course, a caution needs to be noted for the value of r_0 , which should be considered as the apparent size for the source since the emission time between two protons is another folded ingredient. For ^{22}Mg , the source size was extracted to be $r_0 = 2.9 \sim 3.0$ fm, which is a little bit smaller than that of ^{23}Al .

Second, we checked the kinematically complete three-body channels for both ^{23}Al and ^{22}Mg . Figure 3 showed the $C_{pp}(q)$ of the two emitted protons that were coincident with the residues from the mother nuclei. For the channel $^{23}\text{Al} \rightarrow p + p + ^{21}\text{Na}$, Fig. 3(a) showed an almost flat correlation function except for the Coulomb dip in the low- q_{pp} region,

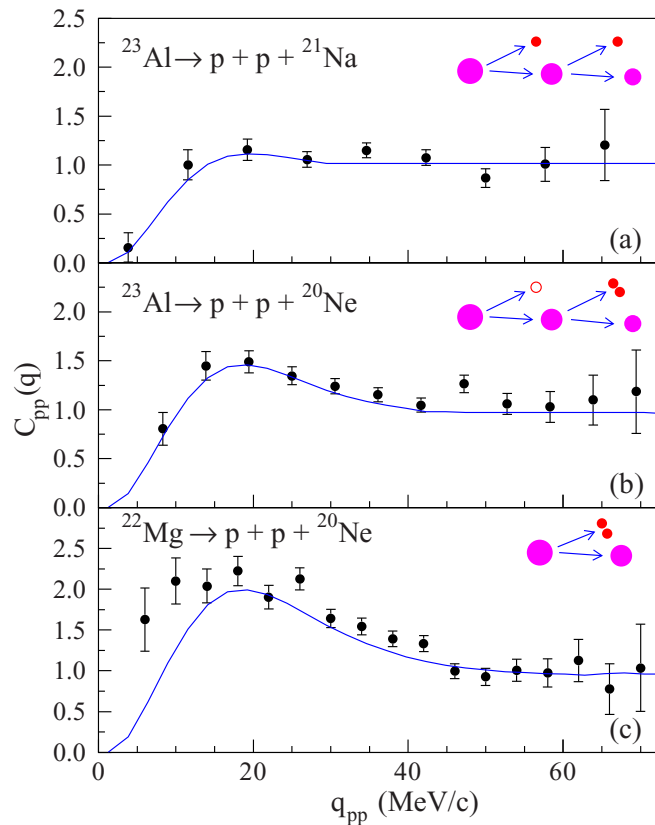


FIG. 3. Same as Fig. 2 but for the reaction channels $^{23}\text{Al} \rightarrow p + p + ^{21}\text{Na}$ (a), $^{23}\text{Al} \rightarrow p + p + ^{20}\text{Ne}$ (b), and $^{22}\text{Mg} \rightarrow p + p + ^{20}\text{Ne}$ (c). Inserts show sketch maps for the most probable emission mechanism.

indicating that the emission of both protons from the ^{23}Al three-body breakup was uncorrelated in phase space except for the Coulomb interaction. This was consistent with the result of no clear observation of diproton emission from the relative momentum and opening angle spectra of ^{23}Al at any excited states [30]. Generally speaking, a flat proton-proton momentum correlation function indicates a very large source size and a very weak two-proton correlation. The $C_{pp}(q)$ data were also compared with the Gaussian source calculations. The fit gave a source size of $r_0 = 3.9 \sim 4.7$ fm, which was larger than that of the inclusive channel of ^{23}Al , indicating a more loose two-proton emission. Because the effect of emission time was not considered, it is difficult to explain the results only by the geometric size of the source.

In contrast, the C_{pp} data for the ^{22}Mg nucleus was very different from that of the ^{23}Al nucleus as shown in Fig. 3(c). In this figure, a strong correlation emerged in C_{pp} spectra for the process of $^{22}\text{Mg} \rightarrow p + p + ^{20}\text{Ne}$, which indicated a compact source size of two-proton emission. The fit gave $r_0 = 2.35 \sim 2.45$ fm, which was smaller than that of the inclusive channel of ^{22}Mg .

Between the two very different two-proton correlation patterns of ^{23}Al and ^{22}Mg , we had checked the intermediate situation. If we looked at the decay process of $^{23}\text{Al} \rightarrow p + p + ^{20}\text{Ne}$, where one proton was not detected by the experimental setup, a moderate correlation appeared at $q_{pp} \sim 20$ MeV/c as shown in Fig. 3(b), which could be understood by assuming the following two-step proton emission process of ^{23}Al . One proton was emitted from ^{23}Al and its corresponding residue nucleus was ^{22}Mg ; Then the other two protons were ejected from ^{22}Mg and its corresponding residue nucleus was ^{20}Ne . Among the three emitted protons, only two protons were detected by the detectors. Because of a strong two-proton correlation in the second step, a moderate two-proton correlation could be eventually observed in the process of $^{23}\text{Al} \rightarrow p + p + ^{20}\text{Ne}$. The peak height of C_{pp} in Fig. 3(b) could be explained by a mixture of Figs. 3(a) and 3(c). The Gaussian source fit gave a size of $r_0 = 3.1 \sim 3.3$ fm, which was between the cases of Figs. 3(a) and 3(c). In addition, to give a visual impression of two-proton emission, the sketch maps were plotted as insets in Fig. 3 to illustrate the most probable emission mechanism for each channel.

The effective source size was extracted from the above analysis. However, it was not clear how the two protons were emitted, i.e., whether the two protons were emitted sequentially or simultaneously. In these two cases, opposite values of the effective source size were observed for ^{23}Al and ^{22}Mg . This indicated that the emission time of protons might be different for these two nuclei. Because time information can also be extracted from the correlation function, it will be very interesting to extract both source size and emission time information. Thus a more general analysis was done for the experimental $C_{pp}(q)$ data. For the different mechanism of two-proton emission, the emission time difference between the two protons is important. Assuming the first proton being emitted at time $t = 0$ and the second proton being emitted at time t , the

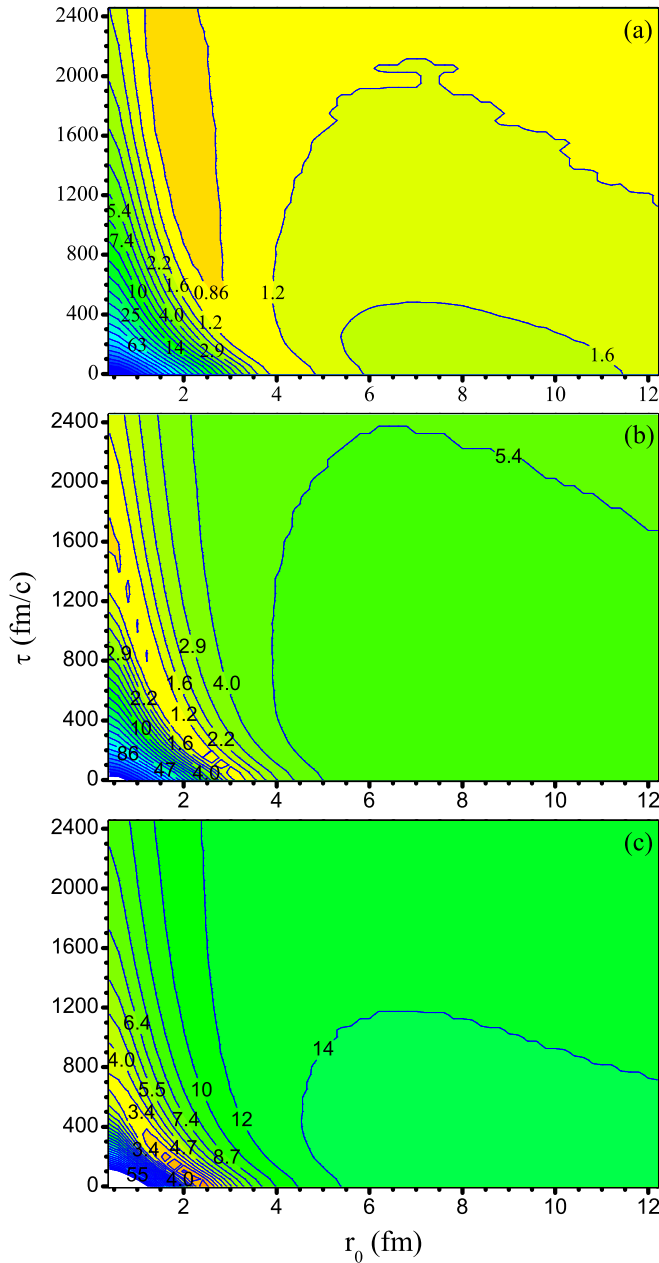


FIG. 4. Contour plot of the reduced χ^2 (χ^2/ν) obtained from fitting the proton-proton momentum correlation function using the CRAB calculation for the reaction channels $^{23}\text{Al} \rightarrow p + p + ^{21}\text{Na}$ (a), $^{23}\text{Al} \rightarrow p + p + ^{20}\text{Ne}$ (b), and $^{22}\text{Mg} \rightarrow p + p + ^{20}\text{Ne}$ (c).

space and time profile of the Gaussian source was simulated according to the function $S(r, t) \sim \exp(-r^2/2r_0^2 - t/\tau)$ in the CRAB code. τ refers to the lifetime for the emission of the second proton, which starts from the emission time of the first proton. The agreement between the calculation and the $C_{pp}(q)$ data was evaluated by determining the value of the reduced χ^2 . The results were shown in Fig. 4 by a contour plot of χ^2/ν as a function of r_0 and τ . For the reaction channel $^{23}\text{Al} \rightarrow p + p + ^{21}\text{Na}$ as shown in Fig. 4(a), the ranges of source parameters were obtained to be $r_0 = 1.2 \sim 2.8$ fm and $\tau = 600 \sim 2450$ fm/c based on the best χ^2 fit. While for the

reaction channel $^{22}\text{Mg} \rightarrow p + p + ^{20}\text{Ne}$ as shown in Fig. 4(c), the ranges of source parameters were $r_0 = 2.2 \sim 2.4$ fm and $\tau = 0 \sim 50$ fm/c. This means that the emission time differences between two protons for ^{23}Al and ^{22}Mg were quite different. For ^{23}Al , the two protons were emitted at very different times ($\tau > 600$ fm/c); i.e., the mechanism is a sequential emission. For ^{22}Mg , the two protons were emitted almost at the same time ($\tau < 50$ fm/c); i.e., the mechanism was essentially simultaneous. Based on the above results and the q_{pp} and θ_{pp} analysis in Ref. [30], all observables indicate the three-body simultaneous decay mechanism for ^{22}Mg . Moreover, for the excitations around the 14.044 MeV, $T = 2$ state a strong diproton-like component was observed. For the reaction channel $^{23}\text{Al} \rightarrow p + p + ^{20}\text{Ne}$ as shown in Fig. 4(c), the determined source parameters were $r_0 = 0.4 \sim 2.0$ fm and $\tau = 350 \sim 1950$ fm/c, which were also between the above two cases and could be explained by the two-step proton emission process of ^{23}Al .

IV. CONCLUSIONS

In summary, measurement on the proton-proton momentum correlation function was applied to the kinematically complete decay of the two reaction channels, $^{23}\text{Al} \rightarrow p + p + ^{21}\text{Na}$ and $^{22}\text{Mg} \rightarrow p + p + ^{20}\text{Ne}$, in this paper. The experiment was performed at the RIKEN RI Beam Factory. The proton-proton momentum correlation function C_{pp} was obtained by the event-mixing method with an iterative calculation. By assuming a simple Gaussian emission source, the effective source sizes were extracted by comparing the CRAB calculation with the experimental C_{pp} data. Different effective source sizes were obtained for ^{23}Al and ^{22}Mg , which comes from the different mechanism of two-proton emission. In a more general analysis including source size and emission time information, a reasonable source size but completely different emission time for the two protons was extracted. The results indicated that the mechanism of two-proton emission from ^{23}Al was dominantly sequential, while that for ^{22}Mg was mainly three-body simultaneous emission with a strong diprotonlike component at excited states around 14.044 MeV. Based on the previous results [30] and this work, it is possible to distinguish clearly the mechanism of two-proton emission by investigating the proton-proton momentum correlation function, the two-proton relative momentum, and the opening angle distributions. The method presented in this work was applied for the first time to two-proton emitters and was shown to provide new and valuable information on the mechanism of two-proton emission.

ACKNOWLEDGMENTS

We are very grateful to all of the staff at the RIKEN accelerator for providing beams during the experiment. The Chinese collaborators greatly appreciate the hospitality from the RIKEN-RIBS laboratory. This work is supported by the Major State Basic Research Development Program of China under Contract No. 2013CB834405 and the National Natural Science Foundation of China under Contracts No. 11421505, No. 11475244, and No. 11175231.

- [1] R. Hanbry Brown and R. Q. Twiss, *Nature (London)* **178**, 1046 (1956).
- [2] G. Goldhaber, S. Goldhaber, W. Lee, and A. Pais, *Phys. Rev.* **120**, 300 (1960).
- [3] S. E. Koonin, *Phys. Lett. B* **70**, 43 (1977).
- [4] W. G. Lynch *et al.*, *Phys. Rev. Lett.* **51**, 1850 (1983).
- [5] G. Verde, D. A. Brown, P. Danielewicz, C. K. Gelbke, W. G. Lynch, and M. B. Tsang, *Phys. Rev. C* **65**, 054609 (2002).
- [6] C. A. Bertulani, M. S. Hussein, and G. Verde, *Phys. Lett. B* **666**, 86 (2008).
- [7] R. Lednicky and V. L. Lyuboshitz, *Yad. Fiz.* **35**, 1316 (1982) [*Sov. J. Nucl. Phys.* **35**, 770 (1982)].
- [8] M. Lisa, S. Pratt, R. Soltz, and U. Wiedemann, *Annu. Rev. Nucl. Part. Sci.* **55**, 357 (2005).
- [9] Y. Hu, Z. Su, and W. Zhang, *Nucl. Sci. Tech.* **24**, 050522 (2013).
- [10] Y. G. Ma *et al.*, *Phys. Rev. C* **73**, 014604 (2006); *Nucl. Phys. A* **790**, 299c (2007).
- [11] K. Ieki *et al.*, *Phys. Rev. Lett.* **70**, 730 (1993).
- [12] N. A. Orr, *Nucl. Phys. A* **616**, 155 (1997).
- [13] F. M. Marques *et al.*, *Phys. Lett. B* **476**, 219 (2000); *Phys. Rev. C* **64**, 061301(R) (2001).
- [14] Z. Kohley *et al.*, *Phys. Rev. Lett.* **110**, 152501 (2013); E. Lunderberg *et al.*, *ibid.* **108**, 142503 (2012).
- [15] V. I. Goldansky, *Nucl. Phys.* **19**, 482 (1960).
- [16] M. Pfützner, M. Karny, L. V. Grigorenko, and K. Riisager, *Rev. Mod. Phys.* **84**, 567 (2012), and references therein.
- [17] B. Blank and M. Płoszajczak, *Rep. Prog. Phys.* **71**, 046301 (2008), and references therein.
- [18] E. Olsen, M. Pfützner, N. Birge, M. Brown, W. Nazarewicz, and A. Perhac, *Phys. Rev. Lett.* **110**, 222501 (2013).
- [19] K. W. Brown *et al.*, *Phys. Rev. Lett.* **113**, 232501 (2014).
- [20] R. A. Kryger *et al.*, *Phys. Rev. Lett.* **74**, 860 (1995).
- [21] G. Raciti, G. Cardella, M. De Napoli, E. Rapisarda, F. Amorini, and C. Sienti, *Phys. Rev. Lett.* **100**, 192503 (2008).
- [22] V. E. Jacob *et al.*, *Phys. Rev. C* **74**, 045810 (2006).
- [23] A. Gade *et al.*, *Phys. Lett. B* **666**, 218 (2008).
- [24] M. Wiescher *et al.*, *Nucl. Phys. A* **484**, 90 (1988); J. A. Caggiano *et al.*, *Phys. Rev. C* **64**, 025802 (2001).
- [25] X. Z. Cai *et al.*, *Phys. Rev. C* **65**, 024610 (2002).
- [26] D. Q. Fang *et al.*, *Phys. Rev. C* **76**, 031601(R) (2007).
- [27] A. Ozawa *et al.*, *Phys. Rev. C* **74**, 021301(R) (2006).
- [28] M. Wiescher *et al.*, *J. Phys. G* **25**, R133 (1999).
- [29] D. Seweryniak *et al.*, *Phys. Rev. Lett.* **94**, 032501 (2005).
- [30] Y. G. Ma, D. Q. Fang *et al.*, *Phys. Lett. B* **743**, 306 (2015).
- [31] M. Lisa *et al.*, *Phys. Rev. Lett.* **71**, 2863 (1993).
- [32] G. Verde, A. Chbihi, R. Ghetti, and J. Helgesson, *Eur. Phys. J. A* **30**, 81 (2006).
- [33] W. A. Zajc *et al.*, *Phys. Rev. C* **29**, 2173 (1984).
- [34] S. Pratt *et al.*, *Nucl. Phys. A* **566**, 103c (1994).